International Journal of Power Electronics and Drive System (IJPEDS)
Vol. 17, No. 4, December 2026, pp. 2997~3012
ISSN: 2088-8694, DOI: 10.11591/ijpeds.v17.i4.pp2997-3012

Dynamic behavior and control of a fixed-gain LLC resonant converter in grid-connected photovoltaic systems

Nadheer M. Mohammed, Yasir M. Y. Ameen, Basil Mohammed Saied
Department of Electrical Engineering, College of Engineering, University of Mosul, Mosul, Iraq

Article Info

Article history:

Received Feb 8, 2026
Revised Sep 18, 2026
Accepted Oct 4, 2026

Keywords:

Fixed-gain control
Grid-connected PV system
LLC resonant converter
Maximum power point tracking
Soft-switching

ABSTRACT

Grid-connected photovoltaic (PV) systems increasingly employ LLC resonant converters for their soft-switching capability and high efficiency. However, traditional maximum power point tracking (MPPT) needs wide-range frequency control, which leads to deviation from resonance and results in the loss of these benefits. This paper presents a fixed-gain control strategy in which the LLC converter is constrained to operate near its resonant frequency with approximately constant voltage gain, while MPPT is achieved by regulating the PV array voltage rather than the DC link voltage. Unlike predictive and hybrid MPPT methods, it adds no hardware or control degrees of freedom; the same perturb-and-observe algorithm, proportional-integral controller, and voltage-controlled oscillator are used, and only the regulated quantity changes. The complete system, comprising a 126.1 kW PV array, LLC converter, and grid-side inverter, is modelled in MATLAB/Simulink under stepped irradiance (300-1000 W/m²). Results show that fixed-gain operation confines the switching frequency to 76-84 kHz, preserves zero-voltage and zero-current switching across all irradiance levels, and results in reduced distortion of resonant current to 6.8% as compared to 14.5% using wide-range control. The PV-to-grid efficiency rises from 89.7% to 92.4% at 300 W/m² and from 93.6% to 95.1% at 700 W/m², while the DC-link voltage remains within ±6.5% without degrading grid-current quality.

This is an open access article under the CC BY-SA license.

Corresponding Author:

Nadheer M. Mohammed
Department of Electrical Engineering, College of Engineering, University of Mosul
AlMinsaa St, Mosul City, Nineveh Governorate, Iraq
Email: nadheer.23enp6@student.uomosul.edu.iq

1. INTRODUCTION

The rapid expansion of grid-connected photovoltaic (PV) generation has placed increasing demands on power electronic conversion stages to achieve high efficiency, reliable maximum power extraction, and compliant grid interaction under continuously varying environmental conditions. In modern PV systems, the DC–DC conversion stage plays a critical role in conditioning the PV output before grid integration, directly influencing system efficiency, thermal stress, and long-term reliability. From industrial and research point of view, the converter topologies are more and more interested for their high switching frequency, low losses and galvanic isolation characteristics, which have to provide a good control performance over a wide operating range [1]-[3].

The common PV architectures are connected to the grid and are usually comprised of a pulse-width-modulated (PWM) DC–DC converter for maximum power point tracking (MPPT) and a voltage source inverter (VSI). PWM converters are well developed and can be easily controlled, but suffer from greater switching losses at higher frequencies, creating the challenge of power density and efficiency at increased

frequencies. The resonant converter, especially LLC topologies, has therefore become a focus of interest for an alternative solution as a result. The ability to achieve zero-voltage switching (ZVS) and zero-current switching (ZCS) results in less switching losses and increased efficiency with high switching frequencies. Such features make LLC resonant converters particularly attractive for high-power and high-density PV applications.

Despite these advantages, adding MPPT to LLC resonant converters is not a trivial task. Unlike duty-cycle-controlled converters, LLC converters rely mainly on frequency modulation to regulate output power. There are traditional MPPT algorithms, such as perturb-and-observe (P&O) and incremental conductance, that are developed for PWM-based converters, and these cannot be applied to resonant converters without changes. The real question is then not whether MPPT can be realized, but rather at what cost, and the only solutions known to date require compromises in tracking performance; either by violating the resonance condition of the converter, or by adding one more degree of freedom, modulation.

Existing attempts to tackle this challenge fall into three clearly distinguishable categories, each with its own drawback. The first is related to frequency modulation of wide range. Within the broader development of grid-connected PV conversion [4], [5], frequency-modulated LLC converters have been reported to achieve MPPT by continuously adjusting the switching frequency in response to irradiance variations [6]. This simplifies the controller while being the very process by which the tank becomes detuned, since when the operating frequency moves away from resonance, the gain curve becomes flat, causing the circulating current to increase and the ZVS condition to be lost.

The second approach keeps the constant switching frequency intact but adds another control degree of freedom – phase shift, PFM-PWM hybrid, or predictive control – to regain the lost regulation capability [7]-[11]. Abdel-Rahim *et al.* [11], for example, do not use any kind of variable frequency in their LLC micro-inverter design through the phase-shifting control of the converter; although the resonant stage is actively controlled, the burden is transferred, not eliminated, and, in the case of prediction-based algorithms, exact system parameter knowledge and extra complexity of the controller are required. Some related work has been performed on multiport and dual-input LLC structures as well as on MPPT improvement [12]-[14]; however, efficiency-focused and alternative modulation approaches [15]-[17] attempt to achieve the same goal through better control of the resonant stage, not through burden offloading. The third approach embraces LLC as a ratio-converting device and moves the burden of regulation somewhere else. Canales *et al.* [18] proved the practicality of the fixed-frequency ZVS LLC with its nearly load-independent transfer characteristic, while Mukherjee *et al.* [19] verified the advantages of using the LLC as the DCX cell compared to the dual active bridge. Wei *et al.* [20] analyzed fixed-frequency LLC stages in two-stage AC/DC converters, where the regulating function belongs to another stage. All of these results show that the resonant stage does not have to regulate — but no-one has considered the situation where the source voltage needs to be changed to achieve maximum power tracking. The other relevant approach involves the DC-link: Zhao *et al.* [21] demonstrated that the deliberate variation of the DC-link voltage helps to increase the performance of the LLC, which proves that the use of the variable DC-link is not a novelty by itself, although in this case it only allows for optimizing the operation of a wide-range converter. Buccella *et al.* [22] are most similar in architecture to the proposed scheme in that both schemes involve LLC converter topology with grid tie together with the outer DC bus loop control along with inner current loop control; however, the purpose is DC bus stiffness along with MPPT where the link voltage is regulated.

As a group, the existing literature contributes three enabling results independently of each other: a fixed frequency operation of the LLC stage with load-independent transfer function, a regulation allocation to a separate converter stage, and the deliberate variation of DC link for improved resonant conditions. However, the missing link in all these contributions is the integration of all three under a single constraint imposed by the PV source, which makes the input voltage a non-design parameter but a result of the MPPT algorithm and I-V characteristics. Thus, in the studies where a fixed ratio was used, the regulated variable remained controllable by the controller, and in grid-connected PV configurations the DC link was intentionally stiffened, which shifted the variation of gain to the resonant stage. Therefore, the missing link is a system-level issue, since none of grid-connected PV topologies studied so far enable a controlled DC link variation to maintain the LLC gain without a special gain regulation loop.

This paper fills this gap with the reallocation of the control task across the two stages, rather than with the use of a new topology or modulation technique. PV array is controlled toward the maximum power point voltage, and LLC converter is allowed to operate in the narrow band around its resonance, to ensure that its conversion gain will be roughly constant; DC-link, in turn, is free to track PV operating point, and the grid-side inverter can absorb any deviation of the latter from the former by varying its current injection level. What is novel in this approach is not the use of fixed-gain LLC operation or variable DC-link control, both of which are well-known practices, but their coordinated interaction with MPPT constraint, which makes the gain regulation loop for the resonant stage unnecessary. It means, in practice, that the proposed method does not require any new hardware, additional sensor, or extra modulation parameter, compared to conventional

wide-range control, with the same P&O algorithm, PI controller, and VCO used. In contrast, predictive MPPT [11] depends on accurate plant parameters, and hybrid PFM–PWM schemes [8], [14] add a second modulation variable. The proposed allocation avoids both, at the cost of a moderate DC-link excursion.

The main contributions of this paper are summarized as follows: i) System-level control coordination scheme for grid-interfaced PV conversion where the DC link is permitted to ride on the PV voltage, allowing the LLC converter to maintain an approximately constant gain without a dedicated gain regulation loop; ii) A detailed analysis of the dynamic behavior of the resonant tank, demonstrating the preservation of ZVS and ZCS characteristics under varying irradiance conditions; iii) An evaluation of the interaction between the fixed-gain LLC converter and the grid-side inverter, with emphasis on DC-link voltage regulation and grid current quality; and iv) Quantitative comparison of fixed-gain and wide-range gain operation with the same controller settings and irradiance profile, reporting frequency deviation, resonant current distortion, magnetizing current variation, maintenance of soft switching, variation in DC-link voltage, and efficiency.

Importantly, the significance of the results described above lies in what they do not require. Improvement in efficiency of resonant photovoltaic power conversion systems is generally achieved via increasing complexity of the control algorithms used, whether through predictive models, hybrid modulations, or auxiliary components, and increases costs and the number of parameters required to implement the system. The present study demonstrates that an equivalent improvement in efficiency under partial irradiance conditions, when most of the operating hours of a photovoltaic plant are spent, is achievable without any change in the control algorithm by simply looking at the variable kept constant. The same MPPT, PI, and VCO controllers are retained, and only the regulated variable is switched from the DC-link voltage to the PV voltage, so the approach can be applied to existing systems without redesign.

The remainder of this paper is organized as follows: i) Section 2 presents the system configuration and modelling of the photovoltaic array and LLC resonant converter; ii) Section 3 describes the proposed control strategy for fixed-gain operation and grid integration; iii) Section 4 discusses the simulation results and comparative performance analysis under dynamic operating conditions; and iv) Finally, section 5 concludes the paper.

2. SYSTEM MODELLING

The proposed grid-connected photovoltaic system consists of a PV array, an LLC resonant DC–DC converter, a three-phase VSI, an LCL filter, and the utility grid. The LLC resonant converter operates as an intermediate power-conditioning stage between the PV array and the inverter, while the inverter ensures grid synchronization and regulated current injection. The overall modelling framework aims to accurately capture the electrical behavior of each subsystem and their interaction under variable operating conditions.

The research design is based on a simulation approach carried out in the MATLAB/Simulink environment. Such an approach is justified for the posed research problem because the research contribution represents a control-level redistribution and not a topological or component-based modification; therefore, the proof of such a contribution would involve comparing two approaches on the same plant, same component parameters, same controller parameters, and same irradiance profile so that any difference found in the presence or absence of soft switching, distortion or efficiency is solely due to the control approach. Such an equivalence is difficult to establish experimentally at this rating because of component tolerances, thermal effects, and layout parasitic. Two operational modes are represented in two versions of the same simulation model, which only differ in the regulated quantity and allowed frequency band, and are exposed to the same stepped irradiance scenario described in section 4.1.

Figure 1 illustrates the schematic of the proposed system. The PV array serves as the primary energy source and delivers a variable DC voltage depending on irradiance and temperature. The LLC resonant converter processes this power and regulates the DC-link voltage supplied to the inverter. In the proposed approach, the LLC converter is operated close to its resonant frequency to maintain approximately constant voltage gain, while the inverter controls the grid current using sinusoidal pulse-width modulation and phase-locked loop synchronization. This separation of roles allows the resonant converter to focus on efficient power conditioning and maximum power extraction, while the inverter ensures compliance with grid voltage, frequency, and power quality requirements.

2.1. PV systems array

The PV array is modelled using the widely adopted single-diode equivalent circuit, which provides an effective balance between modelling accuracy and computational efficiency. Photo-generated voltage is produced due to the separation of opposite charges on both sides of the P-N junction. In the ideal condition without sunlight, a solar cell behaves like a PN junction, and its I-V curve resembles that of a diode. When a reverse voltage is applied, almost no current flows (reverse bias). When a forward voltage is applied, the

current increases gradually and then rises sharply. This behavior corresponds to the physical principle of a PN junction, as illustrated in Figure 2.

The mathematical model of a PV cell is generally based on physical principles and experimental data and primarily describes the current-voltage (I-V) characteristics of the cell. Among the commonly used models, the single diode model is one of the most widely adopted due to its simplicity and broad applicability. The basic form of the equivalent circuit of a photovoltaic cell is shown in Figure 3.

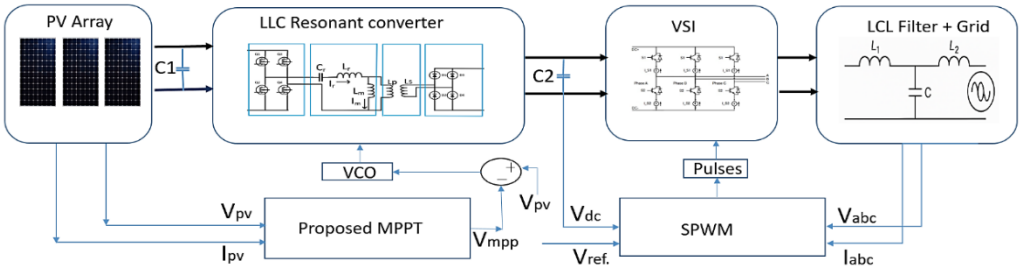

Figure 1. Schematic of the proposed PV system

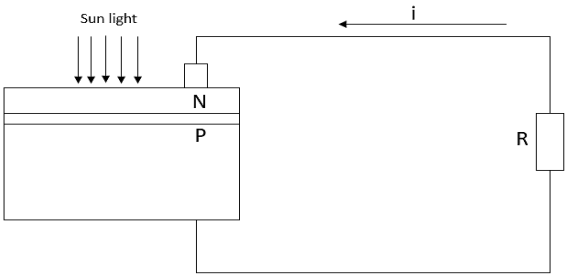

Figure 2. Schematic diagram of the working principle of a photovoltaic cell

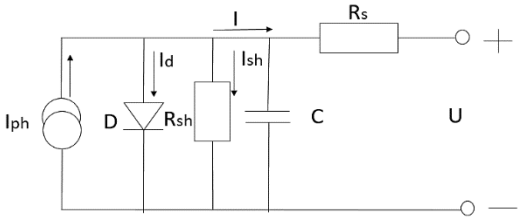

Figure 3. Equivalent circuit of the photovoltaic cell

The series resistance, Rs, is the internal resistance of the cell, and it depends on the resistance of the semiconductor. The shunt resistance, Rsh, is due to leakage at the junction. The I–V characteristic of a PV cell is governed by (1).

$$I = Iph - Is\ [exp\ (^{q\,(Vcell\ +\ RsI)\ /\ BkT)} - 1] - (Vcell + RsI) / Rsh \quad (1)$$

The photovoltaic subsystem consists of a PV array modelled in MATLAB/Simulink. The array is formed by connecting 21 PV modules in series and 15 strings in parallel, yielding a total capacity of 126.1 kW. Each module used in the simulation is based on the performance of the "Jinko Solar Co., Ltd JKM400M-72L-V" panel with a rated power of 400.32 W, a maximum voltage point of 41.7 V, and an open circuit voltage of 49.8 V. Environmental parameters such as solar irradiance and temperature are considered to reflect real operating conditions. Figure 4 illustrates the relationship between the maximum power and the corresponding maximum voltage in a sequential manner.

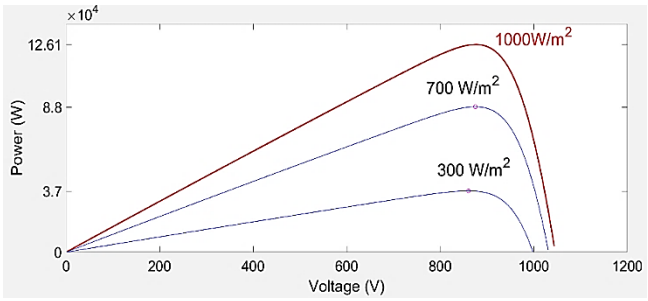

Figure 4. P-V characteristics of the system for Jinko Solar Co., Ltd JKM400M-72L-V module

2.2. LLC resonant converter design

LLC resonant transformers rely on inductive and capacitive reactance, which cancel each other out at a specific frequency, called the resonant frequency. Cancelling the effective reactance at resonance, while keeping internal element resistance to a minimum, to enable efficient power transfer from input to output. The resonant circuit of LLC converters is composed of an inductor and capacitor in series and parallel configurations, enabling flexibility of operations. Therefore, an LLC resonant converter possesses a pair of resonant frequencies.

The first resonant frequency (f_{r1}) depends on the resonant inductor (L_r) and the resonant capacitor (C_r) as obtained in (2). The second resonant frequency (f_{r2}) depends on L_r, C_r, and the magnetizing inductance (Lm) is determined by (3). The equivalent circuit model of LLC is shown in Figure 5. The DC gain of the LLC resonant converter can be obtained, as in (4), based on the fundamental harmonic approximation (FHA) theory [15]:

$$f_{r1} = \frac{1}{2\pi\sqrt{L_r C_r}} \tag{2}$$

$$f_{r2} = \frac{1}{2\pi\sqrt{(L_r+\boldsymbol{Lm})C_r}} \tag{3}$$

$$Gain(G) = \frac{a*V_{oe}}{V_{ge}} = \frac{sLm//Re}{\frac{1}{sCr}+sLr+sLm//Re} \tag{4}$$

where: a is the transformer turns ratio; V_{ge} is the equivalent input voltage; and V_{oe} is the equivalent output voltage.

To simplify (4), the variable Q represents the system's ability to store energy, and mathematically, it is expressed as (5).

$$Q = \frac{X_L}{R_e} = \frac{X_c}{R_e} \tag{5}$$

Re: Reflected resistance represents the reflection of the output load through the transformer to the input side and is mathematically represented as given in (6).

$$Re = \frac{8}{\pi^2} * a^2 * Rout \tag{6}$$

The inductance ratio can be expressed as (7).

$$m = \frac{L_r+Lm}{L_r} \tag{7}$$

Where: L_r is the resonant inductor, Lm is the magnetizing transformer inductance, and C_r is the resonant capacitor.

So, when the power is transferred from the input source V_{ge} to output V_{oe}, it is called forward power transfer, and the gain is expressed in (8).

$$G = \frac{1}{\sqrt{\left(1+\frac{1}{m}\left(1-\frac{1}{f_x^2}\right)\right)^2+\left(f_x-\frac{1}{f_x}\right)^2 Q^2}} \tag{8}$$

Where, F_x is the normalized frequency and is expressed in (9).

Table 1 summarizes the key electrical and resonant parameters of the proposed LLC converter, which are selected to ensure near-resonant fixed-gain operation, adequate soft-switching margin, and stable power transfer across the expected photovoltaic input voltage range. The same component values are used in both operating modes; only the permitted switching frequency range differs, as listed. Keeping the hardware identical ensures that any difference in the results is caused only by the control strategy and not by the converter design.

$$F_x = \frac{f_s}{f_r} \tag{9}$$

So, the point of gain will move according to weather conditions, but it will be near the resonant frequency which it is selected in the proposed design. The gain is a function of the inductance ratio (m), the quality factor (Q), and the normalized frequency (F_x) as shown in Figure 6.

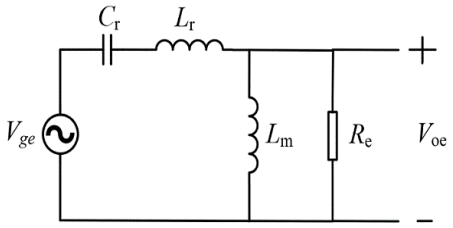

Figure 5. Linear AC circuit model of LLC resonant converter

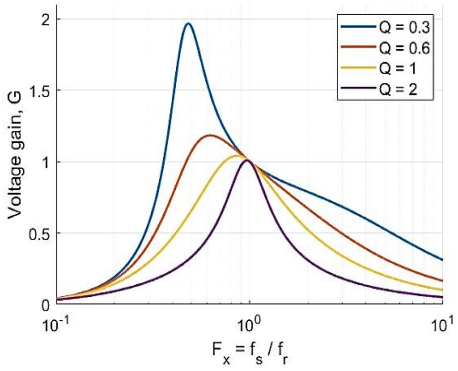

Figure 6. LLC converter gain (G) vs. normalized switching frequency and quality factor

Table 1. Components of the proposed circuit

Parameter	Value	Parameter	Value
Input DC voltage	(750-1050) V	Resonance frequency	80 kHz
DC link nominal	850 V	Switching frequency (wide-range gain mode)	(77-100) kHz
Power	126.1 kW	Switching frequency (fixed-gain mode)	(76–84) kHz
Cr	0.605 µF	m	4
Lr	6.5475 µH	Q	0.6
Lm	20 µH	Transformer ratio	1:1

2.3. Simulation setup and model fidelity

The settings for the control and the settings for the solver are given in Table 2, while the power-stage values are given in Table 1. The PI output is the switching frequency (Hz), which is saturated at 60–100 kHz for both models. Therefore, the 76–84 kHz band obtained under fixed-gain control results from the control allocation and is not an imposed constraint.

There are no losses of switching, core, or winding; ESR losses are neglected, and the losses being modelled are conduction losses that are still less than 0.1 % of rated power reported in section 4, therefore, they are not converter efficiencies. The power measurement takes place at the array terminals as well as the point of common coupling, and the reported value is a PV-to-grid efficiency, which is used here as a relative value between the two allocations. The harmonic content is calculated using the PowerGUI FFT tool: 80 kHz fundamental for the tank current, 50 Hz fundamental up to the 50th order for the grid current. The MPPT perturbation period and step are identical in both models. The comparison reported in section 4 is therefore between the two control allocations under an identical tracking configuration.

Table 2. Control and simulation settings (identical in both modes)

Parameter	Value
PI compensator	Parallel PI, Kp = 500 Hz/V, Ki = 2×10^5 Hz/(V·s)
Frequency-command saturation	60–100 kHz (both modes)
MPPT	P&O, perturbation step 0.5 V, update period 100 µs (identical in both modes)
Semiconductors	Ideal IGBT/diode, Ron = 1 mΩ, Rs = 100 kΩ
DC-link capacitance	1000 µF
Inverter	SPWM, 10 kHz
LCL filter	550 µH / 126 µF / 20 µH (resonance 3.23 kHz)
Solver	ode23t, max step 5 µs, rel. tol. 1×10^-3, 1 s run

3. CONTROL STRATEGY

The control strategy of the proposed grid-connected photovoltaic system is designed to ensure reliable maximum power extraction, stable DC-link voltage behavior, and compliant grid current injection under varying irradiance conditions. For this purpose, a hierarchical control structure is used, where the photovoltaic array, the LLC resonant converter, and the grid-side inverter are coordinated, and there is clear separation of the control tasks. This is the practical implementation of the proposed coordination in section 1, but instead of regulating the voltage by the resonant stage, the regulation process is shared in this way so that the PV array voltage is regulated and the DC-link follows.

The proposed scheme uses the LLC resonant converter as a fixed-gain power conditioning stage around the resonant frequency, and the maximum power point tracking is done by controlling the operating

voltage of the PV array. The grid-side inverter is independently controlled to inject sinusoidal currents in synchronization with the grid, which provides power quality and system stability. This separation of tasks allows each stage to be designed and tuned independently.

3.1. Maximum power point tracking strategy

A P&O algorithm is adopted for maximum power point tracking because of its simplicity, robustness, and applicability to real-time implementation. The proposed system differs from conventional PWM based DC-DC converter, which changes the duty cycle of the PWM directly to achieve MPPT, in that the duty cycle of the PWM is not changed, but instead the operating point of the PV array is controlled by regulating the voltage at the PV array terminals. As a result, the LLC converter can remain close to its resonant point while the MPPT is still achieved.

The P&O algorithm will transiently shake the reference power voltage and monitor the change in output power. If the power has increased, the direction of the perturbation is kept the same; otherwise, it is turned the other way. This process helps the operating point converge towards the maximum power voltage under the steady state conditions and adjust to the changes in the irradiance.

The proposed control scheme uses the output of the MPPT to produce the reference voltage to be used in the control loop of the LLC converter that has as its input command the estimated maximum power point. This voltage based MPPT formulation is very well suited to the fixed-gain LLC operation because it does not require continuous frequency modulation over a large range to track the maximum power, but still allows reliable maximum power tracking. In this way, the MPPT and the LLC control loop are linked through a single voltage reference, which keeps the overall control structure simple.

3.2. Fixed-gain LLC resonant converter control

The LLC resonant converter is controlled to be close to the resonant frequency to have an almost constant voltage gain, and the soft-switching property is maintained. The control strategy would not be to directly control the output voltage of the converter with large frequency changes, but to match the PV operating voltage to the desired resonant operating point. The measured PV voltage is compared to the reference voltage that is calculated by the MPPT algorithm in the control loop.

The resulting error is fed to a proportional-integral (PI) controller whose output sets the switching frequency of the LLC converter within a narrow band around the resonant frequency. This limited frequency adjustment compensates for small variations in operating conditions while preventing significant detuning from resonance. Consequently, the converter retains its high efficiency and soft-switching operation over the full range of irradiance considered.

The block diagram of the LLC control system is illustrated in Figure 7. P&O algorithm control technique is employed widely in the MPPT controllers due to the fact that it is easy to implement and it requires fewer parameters [23]-[26]. MPP of PV modules are tracked by this technique by perturbing iteratively, observing and comparing the PV modules' power output. Perturbation is applied in the operating voltage of the PV module by the P&O technique [27]-[29]. The pulse frequency (PF), obtained from the proposed P&O-based control loop, is the control output instead of the duty cycle in the conventional one. LLC has been designed in a way that it can work with all the inputs of the MPPT approach unit and also to maintain fixed gain and resonant frequency.

In order to compare, the wide-range gain control operating mode is also simulated, where the DC link voltage is kept constant while the frequency of the converter changes over a wider range. The two operating modes are designed using the same resonant tank parameters, PI compensator gains, and MPPT step, making the difference between the two only in the controlled parameter and the allowed range of frequencies.

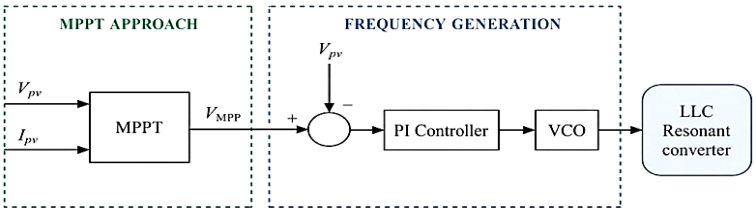

Figure 7. Block diagram of the proposed LLC control system

3.3. Grid-side inverter control

The grid-side inverter is responsible for transferring the conditioned DC power to the utility grid while ensuring compliance with grid codes. A synchronous reference frame control scheme is employed to

regulate the injected grid currents. The three-phase grid voltages are sensed and processed using a phase-locked loop (PLL) to generate the reference angle required for coordinate transformation.

The DC-link voltage is monitored and compared with its reference value. In the fixed-gain mode, the reference value is not a constant but is obtained from the PV operating voltage available from the MPPT stage such that the DC-link tracks the PV operating point and the LLC conversion gain is maintained as a constant. The resulting error is processed through a PI controller to generate the reference active current component. The reactive current reference is set to zero to achieve unity power factor operation. These current references are transformed back to the stationary frame and used to generate the inverter switching signals through sinusoidal pulse-width modulation.

On this basis, the inverter adjusts its current reference to maintain power balance with the fixed-gain LLC converter. This ensures that the power extracted from the PV array is delivered to the grid without accumulating in the DC-link capacitor. The overall control scheme and interaction between the resonant converter and inverter are illustrated in Figure 8. This control structure decouples the grid current regulation from the LLC converter operation, allowing stable grid interaction even when the DC-link voltage experiences moderate variations due to fixed-gain resonant operation.

3.4. Coordination between LLC converter and inverter

The coordination between the LLC resonant converter and the grid-side inverter is critical for ensuring stable system operation. In the proposed architecture, the LLC converter primarily governs power extraction from the PV array, while the inverter adjusts the grid current to match the available DC power. This clear division of roles prevents conflict between the two control loops.

Under fixed-gain operation, the DC-link voltage is allowed to vary within an acceptable range rather than being tightly regulated. This design choice reduces the control burden on the LLC converter and enables resonant-frequency operation. The inverter compensates for these voltage variations by adjusting the injected current magnitude, thereby maintaining stable power transfer to the grid.

For comparative analysis, a wide-range gain control strategy is also implemented, in which the DC-link voltage is tightly regulated by the LLC converter through broad frequency modulation. This alternative approach allows direct evaluation of the impact of gain regulation on resonant behavior, soft-switching performance, and overall system efficiency. The proposed control strategy is designed to achieve the following objectives: i) Accurate tracking of the photovoltaic maximum power point under dynamic irradiance conditions; ii) Preservation of soft-switching characteristics in the LLC resonant converter through near-resonant fixed-gain operation; iii) Stable grid current injection with unity power factor and low harmonic distortion; and iv) Reduced control complexity compared to wide-range frequency modulation approaches.

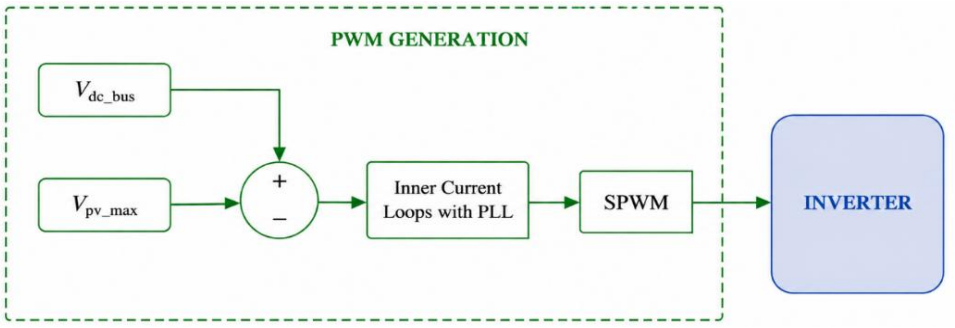

Figure 8. Block diagram of the proposed inverter control system for a fixed-gain LLC converter

4. RESULTS AND DISCUSSION

The performance of the proposed fixed-gain LLC resonant converter control strategy is evaluated using MATLAB/Simulink under dynamic irradiance conditions. The simulation setup follows the system parameters defined in section 2, and the control laws implemented correspond to the MPPT and converter–inverter coordination described in section 3. The two operation methods are analyzed under the same model and the same irradiance profile, and their performances are measured using six criteria: switching frequency deviation, resonant current THD, magnetizing current change, ZVS and ZCS retention, DC-link voltage change, and PV-to-grid efficiency under three irradiance levels. The discussion focuses on the dynamic response of the PV system, resonant tank behavior, soft-switching performance, DC-link voltage dynamics, and grid-side power quality.

4.1. Dynamic response under irradiance variations

To assess the dynamic behavior of the proposed control strategy, the solar irradiance is varied stepwise from 300 W/m² to 700 W/m² and subsequently to 1000 W/m². The irradiance profile applied during the simulation is shown in Figure 9. As governed by the voltage-based perturb-and-observe MPPT algorithm in section 3.1, the PV operating voltage converges toward the corresponding maximum power voltage at each irradiance level. The resulting increase in extracted power is reflected in the resonant current magnitude, while the magnetizing current remains nearly constant. This response is consistent with the LLC resonant tank model presented in section 2.2.

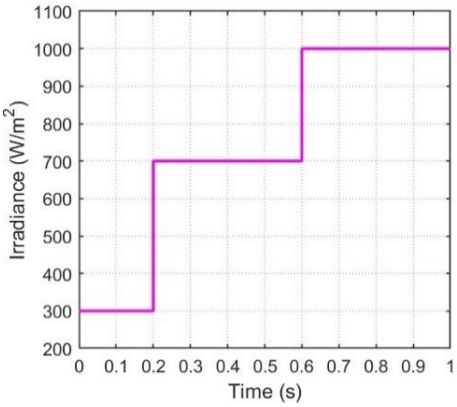

Figure 9. Stepped irradiance profile applied in the simulation

4.2. Resonant tank behavior and soft-switching performance

The waveforms for the tank current under constant gain are given in Figure 10. In Figure 10(a), the square wave input voltage along with the tank current and the magnetizing current can be seen for several switch cycles. Here, the tank current waveform is nearly sinusoidal, and the magnetizing current is nearly triangular, which is characteristic of operation around the resonant frequency.

The respective current characteristics for the entire irradiance range are depicted in Figure 10(b). The value of the resonant current increases for each irradiance step, due to the increase in the amount of harvested energy, while the magnetizing current shape is not affected at all. This is in accordance with the theory described in section 2.2 for the resonant tank configuration, where the value of the magnetizing current depends on the magnetic inductance and the frequency.

In addition, the current through the diode is found to be smooth, unidirectional, and has good zero current intervals as shown in Figure 10(c). Compared with wide-range frequency modulation, the fixed-gain approach keeps the resonant current near sinusoidal and minimizes the circulating current, thereby reducing switching and magnetic losses. This is consistent with the gain properties described in section 2.2, as the near-resonant condition leads to more efficiency. These waveforms also correspond to the envelope stability of the magnetizing current in Figure 10(b), and show that the resonant frequency condition is satisfied during the irradiance series as required by the fixed gain frequency control algorithm.

4.3. Comparison with wide-range gain operation

In order to emphasize the effect of gain regulation on resonant behavior, a wide-range gain operating mode is also studied. The resonant tank waveforms corresponding to this are displayed in Figures 11(a)-11(c). For low irradiance, the current wave form has some distortion and the peaks are flattened, meaning that the current is not operating at the designed resonant frequency.

However, as seen in Figure 11(c), the resonant and magnetizing currents do not cross at the switching instants anymore, which causes partial violation of the soft-switching conditions. This is due to the reduced amplitude of the resonant current at low irradiance, which decreases the resonant tank's ability to completely discharge the parasitic capacitances of the switches prior to commutation. These effects are typical for the gain model presented in section 2.2 and highlight the negative aspects of using wide-range frequency modulation in grid connected applications. The fixed-gain approach depicted in Figure 10, on the other hand, maintains resonant operation for variations in irradiance, exhibiting greater soft switching robustness and better wave shape quality.

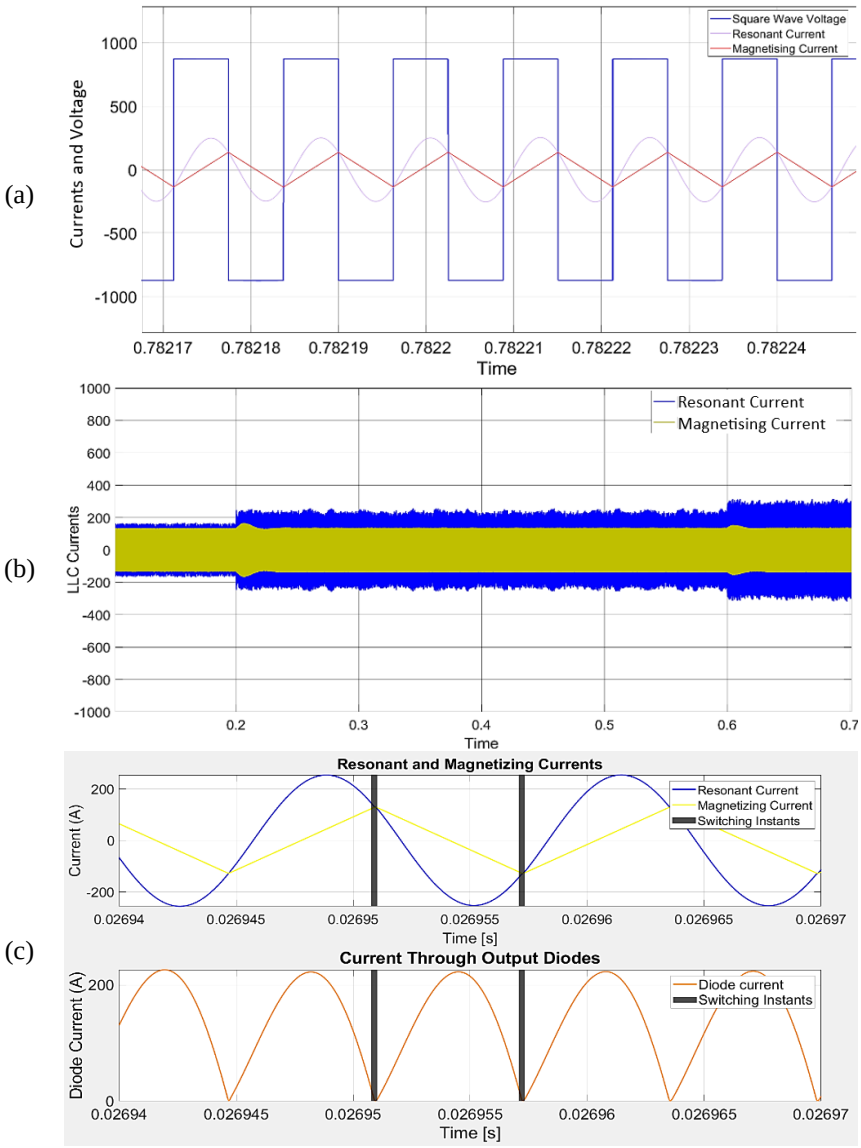

Figure 10. Simulation result of the resonant tank variables in fixed gain technique: (a) LLC converter at resonant, (b) current profile of LLC converter, and (c) instantaneous current waveforms of the resonant tank and output diodes

4.4. DC-link voltage dynamics and converter–inverter interaction

The interaction between the LLC resonant converter and the grid-side inverter is governed by the coordinated control strategy described in section 3.4. Under fixed-gain operation, the DC-link voltage is allowed to vary within an acceptable range rather than being tightly regulated; the aforementioned deviation, shown in Table 3, falls within the range of ±6.5% across the entire irradiance pattern, as opposed to ±2.1% in wide-range gain control. However, the consequences of such regulation are clear from the tank waveforms shown in Figure 11(a); in order to keep the DC link voltage at a steady level, the wide-range controller takes the switching frequency out of resonance, and thus the resonant current loses its almost sinusoidal appearance, while in fixed-gain control the tank stays in resonance and the DC link voltage absorbs all the deviation.

Despite this variation, stable power transfer to the grid is maintained by adjusting the grid current reference according to the power balance relationship. The inverter dynamically compensates for DC-link voltage fluctuations, ensuring continuous and stable current injection. In contrast, wide-range gain operation results in tighter DC-link voltage regulation but introduces significant detuning from resonance, increasing switching stress and reducing overall efficiency. These results highlight a fundamental trade-off between DC-link voltage stiffness and resonant efficiency, emphasizing the importance of coordinated converter–inverter control in grid-connected PV systems.

Table 3. Quantitative comparison of fixed-gain and wide-range gain LLC operation

Performance metric	Fixed-gain LLC operation	Wide-range gain operation
Switching frequency range	76–84 kHz	77–100 kHz
Resonant current THD (300 W/m²)	≈ 6.8%	≈ 14.5%
Grid current THD (700 W/m²)	0.36%	0.33%
Magnetizing current variation	± 3.2%	± 11.6%
ZVS achievement (primary switches)	Maintained across all irradiance levels	Lost at 300 W/m²
ZCS achievement (secondary diodes)	Maintained	Partial loss
DC-link voltage variation	± 6.5%	± 2.1%
Peak resonant current (1000 W/m²)	Normalized 1.0 p.u.	1.05 p.u.
PV-to-grid efficiency (1000 W/m²)	96.2%	95.8%
PV-to-grid efficiency (700 W/m²)	95.1%	93.6%
PV-to-grid efficiency (300 W/m²)	92.4%	89.7%
Switching stress (qualitative)	Low	High
Control complexity	Moderate	High

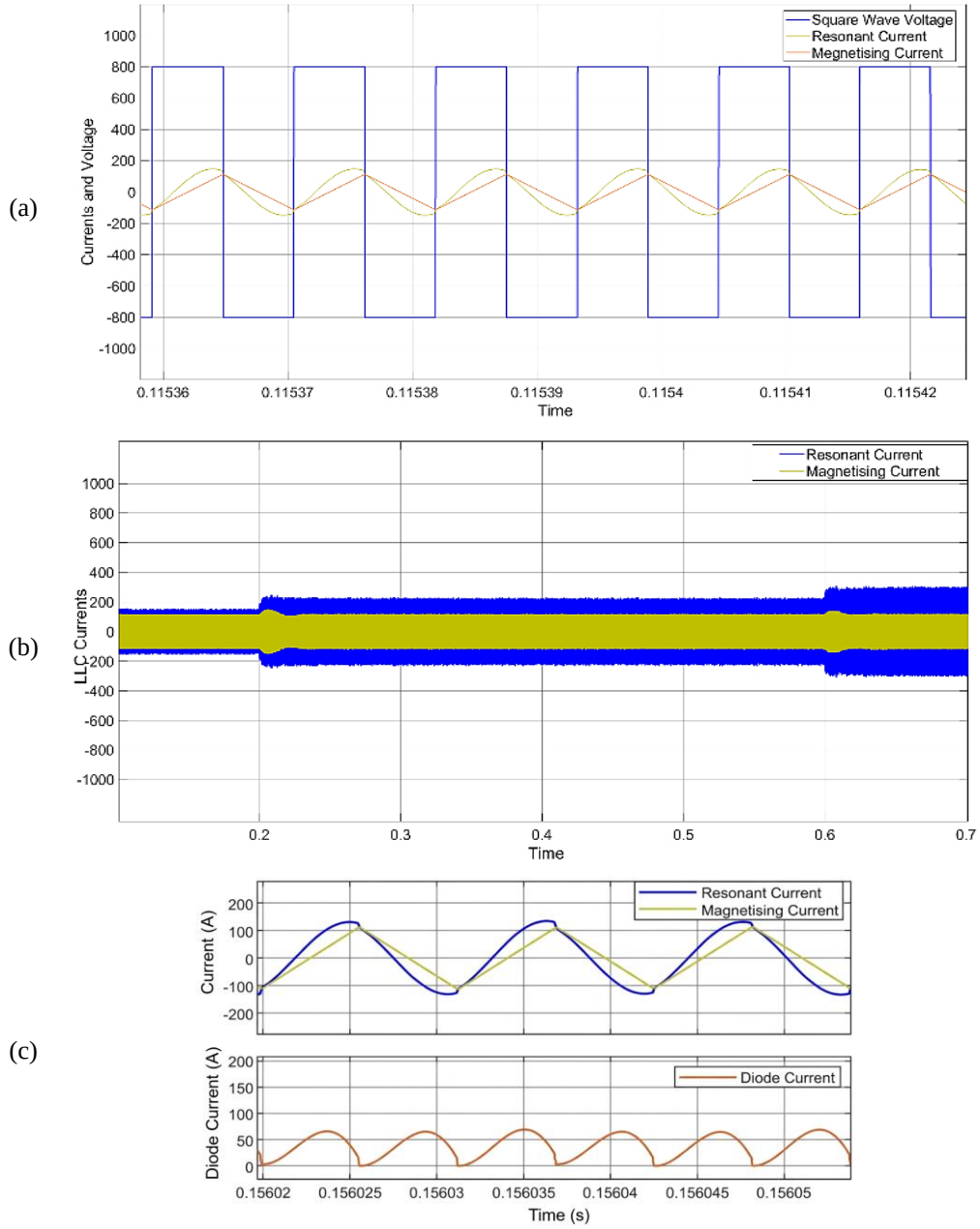

Figure 11. Simulation results of the resonant tank variables in the wide-range gain technique: (a) LLC converter operating away from resonance, (b) current profile of the LLC converter, and (c) instantaneous current waveforms of the resonant tank and output diodes

4.5. Grid-side voltage and current quality

The three-phase grid voltages and currents at the point of common coupling are presented in Figure 12. The results demonstrate that the injected grid currents remain sinusoidal and synchronized with the grid voltage under both fixed-gain and wide-range gain operating modes. Unity power factor operation is achieved by enforcing a zero reactive current reference, as described in section 3.3.

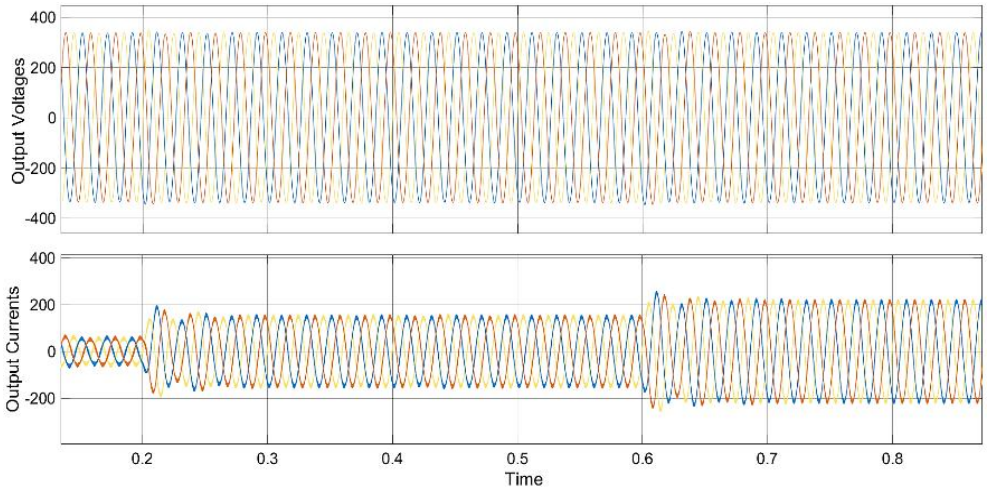

Figure 12. Three-phase grid voltage and current waveforms at the PCC under the stepped irradiance profile

Notably, the differences between the two operating modes are primarily reflected in internal resonant behavior and PV-to-grid efficiency rather than grid-side waveform quality. This indicates that the proposed fixed-gain LLC resonant converter can be effectively integrated into grid-connected PV systems without compromising grid compliance or power quality. This is confirmed by the harmonic analysis below, where the grid-current THD differs by only 0.03% between the two modes.

The uniform resampling of the output of the variable-step solver onto an integer number of fundamental cycles was followed by harmonic analysis of the PCC waveforms for 10 fundamental cycles at 700 W/m². Under fixed-gain operation, the grid-current THD is 0.36%, and under wide-range operation the grid-current THD is 0.33%, while the grid-voltage THD is 0.17% in either case; all the currents are well below the 5% distortion limit of IEEE Std 519-2022 [30]. Note that the two allocations are practically identical at the grid interface, and that their differences remain within the resonant stage. Despite this, the fundamental grid current is still higher for fixed-gain, 161.1 A peak compared to 157.0 A peak at the same irradiance, as reported in section 4.6, which accounts for this as a larger proportion of the array power being fed into the grid.

4.6. Comparative and numerical performance analysis

The performance comparison in Table 3 is quantitative and clearly shows the difference in performance between the proposed fixed-gain LLC operation and the conventional wide-range gain operation. Fixed-gain control restricts the switching frequency to a small range (76-84kHz) around the resonant frequency. This limited frequency excursion is in contrast to the broad operating frequency range of 77- 100 kHz, which is conventionally required, and directly affects the improved resonant behavior and reduced switching stress.

The resonant current total harmonic distortion (THD) under fixed-gain operation is seen to be limited to about 6.8% at low irradiance (300 W/m²), corresponding to the near-sinusoidal current waveform shown in Figure 10(c). On the other hand, the wide-range gain operation has a much larger THD of approximately 14.5%, as is evident in the waveform distortion and current peaks flattening displayed in Figure 11(c). This is a direct result of resonant detuning due to wide frequency modulation.

The stability of the magnetizing current is particularly emphasized. The magnetizing current variation is limited to about ±3.2% when the gain is fixed, while it is ±11.6% when operated in wide ranges. This behavior is similar to the resonant tank model of section 2.2, and is dominated by the resonant frequency and the ratio of inductance. A lower variation means that the magnetic use is improved and core losses are reduced.

Another important differentiating factor is the soft-switching robustness. Fixed-gain operation maintains ZVS of primary-side switches and zero-current switching (ZCS) of secondary-side diodes for all irradiance values tested. However, wide-range gain operation cannot achieve ZVS at 300 W/m² because of the smaller amplitude of resonant current, which is unable to fully discharge the parasitic capacitances of the switch before switching. This loss of soft switching directly increases switching losses and device stress.

The voltage stiffness-resonant efficiency trade-off is observed in the DC-link voltage behavior. Fixed-gain operation allows a DC-link voltage variation of approximately ±6.5%, which is compensated by the grid-side inverter through adaptive current control. Wide-range gain operation achieves tighter regulation, within ±2.1%, but at the expense of resonant detuning and degraded soft-switching performance. The results validate that the variation of the DC-link voltage is moderate enough to be an acceptable and even beneficial design for a grid-connected PV system that uses a resonant converter. It is a variation that is internal; grid compliance is assessed at PCC, with THD of grid current of 0.36%, which is lower than the limit set by IEEE Std 519-2022 [30] of 5% THD. The minimum voltage at the DC-link (≈795 V) is still higher than the minimum linear SPWM requirement (≈653 V) at the 400 V grid. This margin would shrink at high cell temperature and/or with reactive-power support (not studied).

The impact of these operating characteristics is reflected in the overall PV-to-grid efficiency. At the design irradiance of 1000 W/m², both strategies achieve comparable efficiency levels, with fixed-gain operation reaching approximately 96.2% and wide-range gain operation achieving 95.8%. However, under partial irradiance conditions, the superiority of fixed-gain control becomes more pronounced. At 700 W/m², the fixed-gain strategy maintains an efficiency of about 95.1%, compared to 93.6% for the wide-range gain approach. This gap further widens at 300 W/m², where fixed-gain operation achieves approximately 92.4% efficiency, while wide-range gain operation drops to around 89.7%. The differences measured cannot be due to switching-transition or core losses, which are not shown in the model (section 2.3), and they arise instead from the tracking behavior of the two allocations, the less accurate operating point of the array under wide-range operation as the P–V curve flattens at low irradiance. The two effects are, however, working in the same direction for the physical converter—operation away from the series resonance will increase the circulating current and decrease the ZVS, resulting in a more severe efficiency penalty than the difference noted here.

Overall, the comparative analysis confirms that the proposed fixed-gain LLC control strategy offers improved waveform quality, enhanced soft-switching robustness, and higher efficiency under low and medium irradiance conditions, while maintaining acceptable DC-link voltage variation and stable grid interaction. These characteristics make the fixed-gain approach particularly suitable for high-power grid-connected photovoltaic systems, where efficiency, reliability, and thermal performance are critical design considerations.

The findings can be compared to previous LLC-based PV power conversion approaches. The efficiency levels achieved in this study are consistent with the results for efficiency-optimized LLC control in grid-connected inverters [15] and for fixed frequency phase shift modulated LLC micro-inverters [11], which demonstrates that the proposed approach produces equivalent PV to grid efficiency without the use of the additional modulation variable used in those cases. The preservation of ZVS for the entire irradiance range is in agreement with the load-independent transfer function for the fixed-frequency LLC topology [18] and with the fixed conversion ratio behavior for the DCX topology [19], thus demonstrating that the improvement comes from the near-resonant operation regardless of the design used. The main difference is in the DC-link: while [21] changes the link voltage to the optimal value as a design parameter and [22] intentionally makes it stiff in the grid-connected PV system, this study shows that allowing the DC-link to follow the PV operating point within ±6.5% is enough to maintain the resonant operation but still to be fully compensable by the grid-connected inverter as seen from Figure 12.

Table 4 compares the present scheme with the LLC-based approaches discussed in section 1 on the control resources each one consumes and on the resulting frequency span, expressed as the ratio of the highest to the lowest switching frequency required over the operating range. This ratio is used in place of reported efficiency figures, which originate from different ratings, measurement boundaries and loss models and are not directly commensurable.

The frequency span of the proposed allocation (1.11) approaches that of the fixed-ratio converters while retaining maximum power point tracking, which those schemes delegate to a further stage; the wide-range baseline requires 1.30 under identical conditions, and no additional control degree of freedom is introduced. The allocation is therefore confined to applications admitting a moderate DC-link excursion, since a stiff DC-link returns the gain variation to the resonant tank.

Table 4. Comparison with LLC-based PV conversion approaches

Ref.	Resonant stage	Regulating variable	Extra control DoF	f_max/f_min	DC-link
[11]	LLC micro-inverter	Phase shift	Phase-shift angle + predictive MPPT	1.00	Fixed
[15]	LLC, grid-connected inverter	Switching frequency	Efficiency-oriented frequency selection	Not reported	Regulated
[18]	LLC, fixed-frequency ZVS	None (fixed ratio)	—	1.00	Regulated elsewhere
[19]	LLC as DCX cell	None (fixed ratio)	—	1.00	Regulated elsewhere
[21]	LLC with variable DC-link	Switching frequency	DC-link set-point as design variable	Not reported	Varied by design
[22]	LLC, grid-connected PV	DC-link voltage	Outer DC-bus + inner current loops	Not reported	Stiffened
Wide-range (this study)	LLC, grid-connected PV	DC-link voltage	None	1.30	Stiff (±2.1 %)
Proposed	LLC, near-resonant fixed gain	PV array voltage	None (same P&O, PI, VCO)	1.11	Floats with PV point (±6.5 %)

5. CONCLUSION

In this paper, a fixed gain controller for an LLC resonant converter in a grid-connected photovoltaic system was devised, simulated, and compared with traditional wide range gain control. In order to fill the research gap identified in section 1, the regulation was distributed over the two converters, with the photovoltaic array voltage being regulated; the resonant converter was made to operate within a narrow range near the resonant frequency, and the DC-link was made to float at the photovoltaic operation point, with the grid-side inverter making up for the difference. The comparison demonstrated that such a distribution maintains the zero voltage/zero current switching over the entire irradiance range, as opposed to wide-range gain control, which loses the soft switching capability at lower irradiance levels. In addition, the resonant current waveform performance and magnetizing current stability were improved. The key point about the technique is that all these benefits can be achieved without any new component, measurement, or modulation variable in comparison with the conventional one: the only thing that changes is the regulated quantity. It is necessary to mention two restrictions here. First, the results are achieved solely through computer simulation: even though both operation modes have been analyzed for the same model with the same controller parameters (thus making it possible to distinguish the impact of the control technique), semiconductor parasitic, heat dissipation, and electromagnetic interference are not accounted for. Second, the investigation is focused on one particular converter rating and a specific irradiance pattern, which means that the cases of partial shading and abrupt irradiance changes as well as disturbances on the grid side have not been considered yet. Future work will extend the proposed allocation to partial shading, where the multiple maxima of the array characteristic impose large steps in the tracked voltage and thus test the limits within which the tank remains near resonance, and to abrupt irradiance transients and grid-side disturbances. Experimental validation on a reduced-scale prototype is also planned, since the near-resonant operation reported here has not been verified against measured losses. Both allocations would first be tested in controller hardware-in-the-loop and then on the prototype, measuring the switching-frequency span, ZVS, and PV-to-grid efficiency.

FUNDING INFORMATION

No funding involved.

AUTHOR CONTRIBUTIONS STATEMENT

This journal uses the Contributor Roles Taxonomy (CRediT) to recognize individual author contributions, reduce authorship disputes, and facilitate collaboration.

Name of Author	C	M	So	Va	Fo	I	R	D	O	E	Vi	Su	P	Fu
Nadheer M. Mohammed	✓	✓	✓		✓	✓		✓	✓		✓		✓	
Yasir M. Y. Ameen		✓		✓	✓	✓	✓	✓		✓	✓	✓	✓	
Basil Mohammed Saied		✓		✓	✓	✓	✓	✓		✓	✓	✓	✓	

C : **C**onceptualization
M : **M**ethodology
So : **So**ftware
Va : **Va**lidation
Fo : **Fo**rmal analysis
I : **I**nvestigation
R : **R**esources
D : **D**ata Curation
O : Writing - **O**riginal Draft
E : Writing - Review & **E**diting
Vi : **Vi**sualization
Su : **Su**pervision
P : **P**roject administration
Fu : **Fu**nding acquisition

CONFLICT OF INTEREST STATEMENT

We have no known conflicting financial interests or personal relationships that could influence the work reported in this paper.

DATA AVAILABILITY

We confirm that the data supporting the findings of this study are available within the article.

REFERENCES

[1] BPstats, "BP statistical review of world energy," *BP Statistical Review of World Energy*, no. June. London, U.K., pp. 1–48, Jun. 2016. [Online]. Available: https://www.bp.com/en/global/corporate/energy-economics/statistical-review-of-world-energy.html (Accessed: Aug 11, 2020).

[2] K. Kumar, R. Tiwari, P. V. Varaprasad, C. Babu, and K. J. Reddy, "Performance evaluation of fuel cell fed electric vehicle system with reconfigured quadratic boost converter," *International Journal of Hydrogen Energy*, vol. 46, no. 11, pp. 8167–8178, 2021, doi: 10.1016/j.ijhydene.2020.11.272.

[3] K. Kumar, S. R. Kiran, T. Ramji, S. Saravanan, P. Pandiyan, and N. Prabaharan, "Performance evaluation of photo voltaic system with quadratic boost converter employing with MPPT control algorithms," *International Journal of Renewable Energy Research*, vol. 10, no. 3, pp. 1083–1091, 2020, doi: 10.20508/ijrer.v10i3.10800.g7982.

[4] IEA, *Coal 2o18 - analysis and forecasts to 2023*. Paris, France: OECD Publishing, 2018. [Online]. Available: https://www.iea.org/oilmarketreport/.

[5] A. Kumar, N. Gupta, and V. Gupta, "A comprehensive review on grid-tied-solar photovoltaic system," *Journal of Green Engineering*, vol. 7, no. 1, pp. 213–254, Jan. 2017, doi: 10.13052/jge1904-4720.71210.

[6] S. Ghosh, A. Alhatlani, M. Safayatullah, and I. Batarseh, "Review of MPPT methods for LLC converters in photovoltaic applications," in *2022 IEEE Energy Conversion Congress and Exposition, ECCE 2022*, 2022, pp. 1–6, doi: 10.1109/ECCE50734.2022.9947568.

[7] M. N. Alzyod, M. A. Abido, and K. M. Kotb, "MPPT-based optimal frequency control of LLC resonant converter in PV-powered EV charging stations," in *IECON Proceedings (Industrial Electronics Conference)*, 2024, pp. 1–6, doi: 10.1109/IECON55916.2024.10905399.

[8] X. Mao, Q. Huang, Q. Ke, Y. Xiao, Z. Zhe, and M. A. E. Andersen, "Grid-connected photovoltaic micro-inverter with new hybrid control LLC resonant converter," in *IECON Proceedings (Industrial Electronics Conference)*, Florence, Italy, Oct. 2016, pp. 2319–2324, doi: 10.1109/IECON.2016.7793632.

[9] R. Tiwari, K. Kumar, R. B. Neelakandan, S. Padmanaban, and P. W. Wheeler, "Neural network based maximum power point tracking control with quadratic boost converter for PMSG—wind energy conversion system," *Electronics (Switzerland)*, vol. 7, no. 2, 2018, doi: 10.3390/electronics7020020.

[10] K. Kumar, R. Tiwari, N. R. Babu, and K. R. Prabhu, "Analysis of miso super lift negative output Luo converter with MPPT for DC grid connected hybrid pv/wind system," *Energy Procedia*, vol. 145, pp. 345–350, 2018, doi: 10.1016/j.egypro.2018.04.062.

[11] O. Abdel-Rahim, N. Alamir, M. Abdelrahem, M. Orabi, R. Kennel, and M. A. Ismeil, "A phase-shift-modulated LLC-resonant micro-inverter based on fixed-frequency predictive MPPT," *Energies*, vol. 13, no. 6, p. 1460, 2020, doi: 10.3390/en13061460.

[12] Y. Wang and L. Sun, "Photovoltaic maximum power point tracking technology based on improved perturbation observation method and backstepping algorithm," *Electronics (Switzerland)*, vol. 13, no. 19, Oct. 2024, doi: 10.3390/electronics13193960.

[13] G. Jean-Pierre, A. El Shafei, N. Altin, and A. Nasiri, "A multiport bidirectional LLC resonant converter for grid-tied photovoltaic-battery hybrid system," in *International Journal of Renewable Energy Research*, Brasov, Romania, 2020, pp. 862–870, doi: 10.20508/ijrer.v10i2.10308.g7953.

[14] X. Chen and I. Batarseh, "PWM and PFM hybrid modulation scheme for dual-input LLC resonant converter," in *ECCE 2020 - IEEE Energy Conversion Congress and Exposition*, 2020, pp. 2569–2576, doi: 10.1109/ECCE44975.2020.9235878.

[15] C. Hisar, N. Altin, S. Ozdemir, and I. Sefa, "Efficiency-oriented control of LLC resonant converter for grid-connected inverter," *IET Renewable Power Generation*, vol. 19, no. 1, pp. 1–14, 2025, doi: 10.1049/rpg2.70050.

[16] O. Kwon, K. S. Kim, and B. H. Kwon, "Highly efficient single-stage dab microinverter using a novel modulation strategy to minimize reactive power," *IEEE Journal of Emerging and Selected Topics in Power Electronics*, vol. 10, no. 1, pp. 544–552, Feb. 2022, doi: 10.1109/JESTPE.2021.3090097.

[17] S. Necaibia, M. S. Kelaiaia, H. Labar, A. Necaibia, and E. D. Castronuovo, "Enhanced auto-scaling incremental conductance MPPT method, implemented on low-cost microcontroller and SEPIC converter," *Solar Energy*, vol. 180, pp. 152–168, 2019, doi: 10.1016/j.solener.2019.01.028.

[18] F. Canales, P. Barbosa, and F. C. Lee, "A wide input voltage and load output variations fixed-frequency ZVS DC/DC LLC resonant converter for high-power applications," *Conference Record - IAS Annual Meeting (IEEE Industry Applications Society)*, vol. 4, pp. 2306–2313, 2002, doi: 10.1109/IAS.2002.1042768.

[19] S. Mukherjee, A. Kumar, and S. Chakraborty, "Comparison of DAB and LLC DC-DC converters in high-step-down fixed-conversion-ratio (DCX) applications," *IEEE Transactions on Power Electronics*, vol. 36, no. 4, pp. 4383–4398, Apr. 2021, doi: 10.1109/TPEL.2020.3019796.

[20] T. Wei, A. Cervone, and D. Dujic, "Second harmonic induced resonant modes of fixed-frequency operated LLC converters," *IEEE Transactions on Industry Applications*, vol. 61, no. 4, pp. 6547–6555, 2025, doi: 10.1109/TIA.2025.3548605.

[21] S. Zhao, A. Kempitiya, W. T. Chou, V. Palija, and C. Bonfiglio, "Variable DC-link voltage LLC resonant dc/dc converter with wide bandgap power devices," *IEEE Transactions on Industry Applications*, vol. 58, no. 3, pp. 2965–2977, May 2022, doi: 10.1109/TIA.2022.3151867.

[22] C. Buccella, C. Cecati, H. Latafat, and K. Razi, "A grid-connected PV system with LLC resonant DC-DC converter," in *4th International Conference on Clean Electrical Power: Renewable Energy Resources Impact, ICCEP 2013*, Alghero, Italy, 2013, pp. 777–782, doi: 10.1109/ICCEP.2013.6586947.

[23] C. Abdelkhalek, E. B. Said, and A. Younes, "A novel MPPT tactic for PV systems with fast-converging speed and zero oscillation," in *2020 5th International Conference on Renewable Energies for Developing Countries, REDEC 2020*, 2020, pp. 1–6, doi: 10.1109/REDEC49234.2020.9163606.

[24] J. Liu, J. Zhang, T. Q. Zheng, and J. Yang, "A modified gain model and the corresponding design method for an LLC resonant converter," *IEEE Transactions on Power Electronics*, vol. 32, no. 9, pp. 6716–6727, Sep. 2017, doi: 10.1109/TPEL.2016.2623418.
[25] A. H. Mutlag, A. Mohamed, and H. Shareef, "An improved perturbation and observation based maximum power point tracking method for photovoltaic systems," *Jurnal Teknologi*, vol. 78, no. 6–2, pp. 19–25, 2016, doi: 10.11113/jt.v78.8887.
[26] F. Liu, Y. Kang, Z. Yu, and S. Duan, "Comparison of P&O and hill climbing MPPT methods for grid-connected PV converter," in *2008 3rd IEEE Conference on Industrial Electronics and Applications, ICIEA 2008*, Singapore, Jun. 2008, pp. 804–807, doi: 10.1109/ICIEA.2008.4582626.
[27] W. Wang, Y. Liu, J. Zhao, Q. Yin, Q. Lv, and P. Zhang, "Output current ripple and efficiency optimal control method for multi-phase interleaved LLC resonant converter," *Frontiers in Energy Research*, vol. 10, 2022, doi: 10.3389/fenrg.2022.870760.
[28] G. Yao, Z. Luo, Z. Lu, M. Wang, J. Shang, and J. M. Guerrerob, "Unlocking the potential of wave energy conversion: a comprehensive evaluation of advanced maximum power point tracking techniques and hybrid strategies for sustainable energy harvesting," *Renewable and Sustainable Energy Reviews*, vol. 185, 2023, doi: 10.1016/j.rser.2023.113599.
[29] K. Krishnamurthy, S. Padmanaban, F. Blaabjerg, R. B. Neelakandan, and K. R. Prabhu, "Power electronic converter configurations integration with hybrid energy sources–a comprehensive review for state-of the-art in research," *Electric Power Components and Systems*, vol. 47, no. 18, pp. 1623–1650, 2019, doi: 10.1080/15325008.2019.1689457.
[30] IEEE, "IEEE standard for harmonic control in electric power systems," *IEEE Std 519-2022 (Revision of IEEE Std 519-2014)*. pp. 1–31, 2022.

BIOGRAPHIES OF AUTHORS

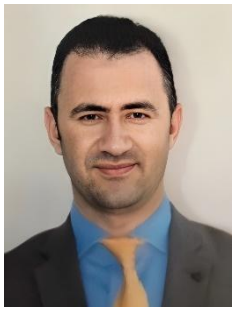

Nadheer M. Mohammed received his Bachelor of Science (B.Sc.) degree in electrical engineering from the University of Diyala, Iraq, in 2005, and his Master of Science (M.Sc.) degree in electrical engineering, specializing in power and machines, from Tikrit University, Iraq, in 2022. He is currently pursuing a Doctor of Philosophy (Ph.D.) degree in the Department of Electrical Engineering, College of Engineering, University of Mosul, Mosul, Iraq. He works as a chief engineer at the Iraqi Ministry of Oil. His research interests include grid-connected photovoltaic systems, power electronic converters, and electrical machines. He can be contacted at email: nadheer.23enp6@student.uomosul.edu.iq.



Dr. Yasir M. Y. Ameen received his bachelor's, master's, and Ph.D. degrees in power and electrical machines engineering from the University of Mosul, Iraq, in 1997, 2000, and 2008, respectively. He is a member of the Iraqi Engineers Union (IEU) and a lecturer in the Department of Electrical Engineering. His research interests include power electronics, electrical machines, and their drives. His affiliation is the Department of Electrical Engineering, College of Engineering, University of Mosul, Mosul 41001, Iraq. He can be contacted at email: yasir_752000@uomosul.edu.iq.



Prof. Dr. Basil Mohammed Saied received his Ph.D. degree from the University of Bath, United Kingdom, his M.Sc. degree from the University of Bradford, United Kingdom, and his B.Sc. degree from the University of Mosul, Iraq. He was formerly a professor in the Department of Electrical Engineering at the University of Mosul. His major research interests include power electronics, electric drives, power quality, and electrical machines. He is affiliated with the Department of Electrical Engineering, College of Engineering, University of Mosul, Mosul 41001, Iraq. He can be contacted at email: basil.al.hashimie@uomosul.edu.iq.